Available online at www.sciencedirect.com
SCIENCE DIRECT®
Journal of Catalysis 225 (2004) 327–336
JOURNAL OF CATALYSIS
www.elsevier.com/locate/jcat

Effect of morphological characteristics of TiO_2-supported noble metal catalysts on their activity for the water–gas shift reaction

Paraskevi Panagiotopoulou and Dimitris I. Kondarides *

Department of Chemical Engineering, University of Patras, GR-26504 Patras, Greece

Received 15 March 2004; revised 20 April 2004; accepted 24 April 2004

Abstract

The catalytic activity of M/TiO_2 catalysts (M = Pt, Rh, Ru, Pd) for the water–gas shift (WGS) reaction has been investigated in the temperature range of 150–450 °C with respect to the structural and morphological properties of the dispersed metallic phase and the support. It has been found that the turnover frequency (TOF) of CO conversion varies in the order of Pt > Rh > Ru > Pd, with Pt being about 20 times more active than Pd. The activation energy of the reaction is practically the same for all metals examined. Conversion of CO at a given temperature increases significantly with increasing metal loading in the range of 0.1–5.0 wt%. However, activation energy and TOF do not depend on the morphological and structural characteristics of the metallic phase, such as loading, dispersion, and crystallite size. This has been clearly shown in the case of Pt/TiO_2 catalysts, where the TOF of CO conversion was found to be independent of the Pt crystallite size in the range of 1.2 to 16.2 nm. The effect of the morphology of the support on catalytic performance has been investigated over Pt catalysts supported on four commercial titanium dioxide carriers with different structural characteristics (surface area, primary crystallite size of TiO_2). It has been found that conversion of CO at low temperatures (< 300 °C) is significantly improved when Pt is dispersed on TiO_2 samples of low crystallite size. The turnover frequency of CO increases exponentially with decreasing the primary crystallite size of TiO_2, accompanied by a substantial decrease of the apparent activation energy of the reaction. In particular, the rate per surface Pt atom increases by more than two orders of magnitude with decreasing crystallite size of TiO_2 from 35 to 16 nm, with a parallel decrease of activation energy from 16.9 to 11.9 kcal/mol. It is concluded that noble metal catalysts highly dispersed on titanium dioxide carriers with small TiO_2 crystallite size are promising candidates for use in low-temperature WGS reactors for fuel cell applications.

Keywords: Water–gas shift; Noble metal catalysts; TiO_2; Morphological properties

1. Introduction

The water–gas shift (WGS) reaction is an important step in a number of chemical processes, typically employed for the production of hydrogen by conversion of carbon monoxide in the presence of water:

$$CO + H_2O \leftrightarrow CO_2 + H_2, \quad \Delta H = -41.1 \text{ kJ/mol}.$$

The WGS technology is well established and widely used in large-scale steady-state operations, such as hydrogen or ammonia plants. The reaction is moderately exothermic and equilibrium limited and, therefore, low CO levels can only be achieved at low temperatures, however, with favorable kinetics at higher temperatures. As a result, two WGS reactors are typically employed in industry: a high-temperature shift (HTS) reactor, operating at 350–450 °C, for rapid CO conversion, and a low-temperature shift (LTS) reactor, operating at 180–250 °C, for achievement of lower equilibrium CO contents. Conventional HTS catalysts, usually Fe–Cr oxide, are inactive at temperatures below 300 °C, while Cu–ZnO–Al_2O_3 catalyst formulations, used for LTS reaction, degrade above 250 °C.

The interest for the WGS reaction has grown significantly in the last few years, as a result of the advancements in fuel cell technology and the need for developing fuel processors capable of converting carbonaceous fuels into hydrogen [1,2]. A fuel processor typically consists of a reformer, which converts the fuel into a hydrogen-rich gas stream, and a water–gas shift unit, which converts by-product carbon monoxide into additional hydrogen. In certain cases, as

* Corresponding author. Fax: +30 2610 997853.
E-mail address: dimi@chemeng.upatras.gr (D.I. Kondarides).

0021-9517/$ – see front matter
doi:10.1016/j.jcat.2004.04.030

in polymer electrolyte membrane (PEM) fuel cell applications, an additional cleanup step, e.g., preferential oxidation (PROX) or methanation, is required to reduce CO levels to less than 50 ppm, as dictated by the poisoning limit of the Pt electrodes [1,2]. In such cases, the WGS catalyst should be active at temperatures in the range of 200–280 °C, depending on the inlet gas composition, in order to be able to reduce CO concentration to the desired level (0.5–1.0%) [2].

Conventional industrial catalysts cannot be used for mobile and small-to-medium-scale fuel cell applications for power generation, mainly due to restrictions in volume, weight, and cost. In addition, Fe–Cr and Cu–ZnO–Al_2O_3 catalysts are pyrophoric and must be sequestered during system shutdown when only air flows through the system. Furthermore, both catalysts need to be carefully activated before use, requiring lengthy preconditioning steps. It is, therefore, evident that novel WGS catalysts need to be developed to meet the necessary criteria for use in fuel processors. Noble metal catalysts may offer significant advantages compared to conventional ones, including high activity at a wider temperature range, no need of activation prior to use, no degradation on exposure to air or temperature cycles, and availability of conventional wash-coating technologies, which may result in reduced size and weight and improved ruggedness.

The WGS reaction has been investigated over a variety of metal catalysts, including Pt [3,4], Rh [3–5], Ru [3,6], Pd [3,7], Au [3,8–11], Re [3], Os [3], Ir [3,12], Ag [10], Cu [3,10,13], Ni [3,7,13], Fe [3,7], and Co [3,7], supported on oxide and mixed oxide supports. Among the various metal–support combinations examined so far, the Pt/CeO_2 catalyst seems to be a promising candidate, characterized by high activity at low-to-medium reaction temperatures. However, recent studies under conditions typical of a reformer outlet showed a progressive deactivation of ceria-supported noble metals [14]. This has been attributed to the irreversible reduction of the support [14] and/or to structural changes and sintering of the metallic phase [15,16].

A detailed investigation is being carried out in this laboratory in an attempt to identify the key parameters that determine the catalytic activity of supported noble metal catalysts for the WGS reaction and to explore the mechanism of the reaction. The aim is to develop stable LT-WGS catalysts sufficiently active at reaction temperatures lower than 250 °C. In the present study, the effect of structural and morphological characteristics of the dispersed metallic phase and the support is investigated over Pt, Rh, Ru, and Pd catalysts supported on titanium dioxide carriers.

2. Experimental

2.1. Catalyst preparation

Catalysts were prepared by impregnation of titanium dioxide powder with an aqueous solution of the corresponding metal precursor salt ($Rh(NO_3)_3$, $Ru(NO)(NO_3)_3$, $(NH_3)_2Pt(NO_2)_2$, and $(NH_3)_2Pd(NO_2)_2$). The resulting slurry was heated slowly at 70 °C under continuous stirring and maintained at that temperature until nearly all the water evaporated. The solid residue was dried at 110 °C for 24 h and then reduced at 300 °C (400 °C for Ru catalysts) in H_2 flow for 2 h. The metal loading of the catalysts thus prepared varied between 0 and 5 wt%. In certain cases, where catalysts with large Pt crystallites were desired, the dried samples were calcined in air at 600 or 700 °C for a period of 2 or 4 h and then reduced in H_2 as described above. In most cases, the TiO_2 carrier used for catalyst preparation was Degussa P25. Three more types of commercial TiO_2 powders, denoted as UV, PC, and AT (see Table 1 for notations), were used to study the effect of morphological characteristics of the support on the WGS activity of Pt catalysts.

2.2. Catalyst characterization

Specific surface areas of supports and catalysts were measured with the BET technique with the use of a Micromeritics (Gemini III 2375) instrument, employing nitrogen physisorption at the temperature of liquid nitrogen. Prior to each measurement, the sample was dried at 120 °C under helium flow passing through the sample cell.

X-ray diffraction (XRD) patterns of bare and metallized titanium dioxide samples were obtained on a Philips P (PW

Table 1
Phase composition, primary crystallite size, and specific surface area of TiO_2 supports and 0.5% Pt/TiO_2 catalysts

Product	TiO_2 (as-received powder)				0.5% Pt/TiO_2			
	Notation	Composition (% anatase)	TiO_2 crystal size (nm)	Surface area (m^2/g)	Fresh catalyst		Conditioned catalyst	
					TiO_2 crystal size (nm)	Surface area (m^2/g)	TiO_2 crystal size (nm)	Surface area (m^2/g)
Hombikat UV-100 Sachtleben Chemie	UV	100	~9	238	12	104	16	71
PC-500 Millennium Chemicals	PC	100	~9	159	11	111	18	64
P-25 Degussa	P25	75	23	41	25	41	25	39
AT-1 Millennium Chemicals	AT	100	30	8	33	8	35	8

1830/40) powder diffractometer. Scans were collected in the range of 2θ between 20 and 80° with a scanning rate of 0.05°/s. The ratio (x_A) of anatase in the TiO_2 samples was estimated using [17]

$$x_A = \left[1 + 1.26(I_R/I_A)\right]^{-1}, \quad (1)$$

where I_A and I_R are the integral intensities of the anatase (101) and rutile (110) reflections, respectively. The primary crystallite size of TiO_2 (d_{TiO_2}) was calculated by means of Scherrer's equation [18],

$$d_{TiO_2} = \frac{0.9\lambda}{B\cos\theta}, \quad (2)$$

where λ is the X-ray wavelength corresponding to Cu-K_α radiation (0.15406 nm), B is the broadening (in radians) of the anatase (101) reflection, and θ is the angle of diffraction corresponding to the peak broadening. It should be noted that d_{TiO_2} refers to the average size of the individual crystalline domains, rather than the size of particles formed by the agglomeration of crystals. As a result, the term *primary crystallite size* used here indicates the X-ray-scattering domain size which may or may not correspond to physical particle dimensions.

Catalysts were characterized in terms of their dispersion and mean crystallite size by H_2 chemisorption at 25 °C for Pt and Rh, 60 °C for Pd, and 100 °C for Ru samples. Adsorption isotherms were obtained with the volumetric technique in the pressure range of 0–75 Torr employing a modified Fisons Instruments (Sorptomatic 1900) apparatus. Prior to each measurement, the catalyst sample (ca 1.0 g) was pretreated by (a) dynamic vacuum at 250 °C for 1 h; (b) reduction with 1 bar of H_2 at 250 °C for 1 h, (c) evacuation for 30 min at 250 °C, and (d) cooling down to the chemisorption temperature. The hydrogen uptake at monolayer coverage was obtained for each catalyst by extrapolation of the adsorption isotherm to zero pressure. The exposed surface area of metal M (M = Pt, Ru, Rh, Pd) was calculated assuming a H:M stoichiometry of 1:1, and an atomic surface area of 8.9 Å^2 for Pt, 8.6 Å^2 for Ru, 7.6 Å^2 for Rh, and 7.8 Å^2 for Pd. The crystallite sizes of the dispersed metals were estimated from the H_2 chemisorption data, assuming spherical particles, using the relation,

$$d_M = \frac{6}{\rho_M S_M}, \quad (3)$$

where d_M is the mean crystallite diameter, S_M is the surface area per gram of metal, and ρ_M is the density of metal M.

2.3. Catalytic performance tests and kinetic measurements

Catalytic performance tests have been carried out using an apparatus which consists of a flow measuring and control system, the reactor, and an on-line analysis system. The flow system is equipped with a set of mass-flow controllers (MKS) to control the flow and composition of the inlet gases (CO, H_2, He), a syringe pump (Braintree Scientific Inc.), which is used for feeding water, and a set of valves, which allows selection of gas feed composition and introduction of the gas mixture to the reactor or to a by-pass loop stream. Water is pumped into a vaporizer where it is vaporized and heated to 170 °C and mixed with the gas stream coming from the mass-flow controllers. The resulting gas mixture is then fed to the reactor through stainless-steel tubing maintained at 150 °C by means of heating tapes.

The reactor consists of a 25-cm-long quartz tube (6 mm o.d.) with an expanded 1-cm-long section in the middle (8 mm i.d.), in which the catalyst sample is placed. Reaction temperature is measured in the middle of the catalyst bed by means of a K-type thermocouple placed within a quartz capillary well, which runs through the cell. The reactor is placed in an electric furnace, the temperature of which is controlled using a second K-type thermocouple placed between the reactor and the walls of the furnace. A pressure indicator is used to measure the pressure drop in the catalyst bed.

The analysis system consists of a gas chromatograph (Shimadzu) interfaced to a personal computer. The chromatograph is equipped with two packed columns (Porapak-Q, Carboxen) and two detectors (TCD, FID) and operates with He as the carrier gas. The injection of the gas mixture to the desired column is achieved by means of two six-port valves heated at 150 °C. Determination of the response factors of the detectors has been achieved with the use of gas streams of known composition (Scott specialty gas mixtures). Reaction gases (He, 10%CO/He, H_2) are supplied from high-pressure gas cylinders (Messer Griesheim GMBH) and are of ultrahigh purity.

In a typical experiment, an amount of 100 mg of fresh catalyst ($0.18 < d < 0.25$ mm) is placed in the reactor and reduced in situ at 300 °C for 1 h under a hydrogen flow of 60 cc/min. The catalyst is then heated at 500 °C under He flow and left at that temperature for 15 min. Finally, temperature is lowered to 450 °C and the flow is switched to the reaction mixture, which consists of 3% CO–10% H_2O in He. The catalyst is conditioned at this temperature for 1 h and then the conversions of reactants and products are determined using the analysis system described above. Similar measurements are obtained following a stepwise lowering of temperature, until conversion of CO drops close to zero. A few more measurements are then obtained by stepwise increasing temperature to check for possible catalyst deactivation. In all cases, data points are averages of at least three measurements. All experiments were performed at near atmospheric pressure.

Measurements of reaction rates were obtained in separate experiments where the conversions of reactants were kept below 10% so that differential reaction conditions could be assumed, with negligible heat and mass-transfer effects. Rates were calculated using the following expression,

$$r_{CO} = \frac{(C_{CO}^{in} - C_{CO}^{out})F}{W}, \quad (4)$$

where r_{CO} is the conversion rate of CO (mol s^{-1} g_{cat}^{-1}), F is the total flow rate (mol s^{-1}), W the mass of catalyst (g), and C_{CO}^{in}, C_{CO}^{out} are the inlet and outlet concentrations of CO, respectively. These results, along with the measurements of metal dispersion, were used to calculate the turnover frequencies (TOFs) of carbon monoxide, defined as moles of CO converted per surface metal atom per second (s^{-1}),

$$\mathrm{TOF} = \frac{r_{CO} AB_M}{D X_M}, \tag{5}$$

where AB_M represents the atomic weight of metal M, X_M the metal content (g_{met}/g_{cat}), and D the metal dispersion.

It should be noted that rates were highly reproducible as can be evidenced from the TOFs measured over the 0.5% Pt/TiO_2 catalyst (Fig. 4, vide infra), which correspond to measurements obtained from four different experiments conducted during the period of the present study.

3. Results and discussion

3.1. Physicochemical characteristics of supports and catalysts

The diffractograms obtained from the as-received titanium dioxide powders used as supports are shown in Fig. 1. It is observed that, with the exception of P25 which contains 25% rutile, all samples consist of TiO_2 in its anatase form. The primary crystallite size of TiO_2, determined by XRD peak broadening, and the BET surface area of the powders vary significantly from one sample to another, ranging from 9 nm (238 m^2/g) for UV to 30 nm (8 m^2/g) for AT (Table 1). Interestingly, the as-received UV and PC samples, although having similar primary crystallite size ($\sim$ 9 nm), possess significantly different BET surface areas (238 and 159 m^2/g, respectively). This is most likely due to the higher degree of crystallite aggregation in the PC sample and the formation of clusters, which results in lower microporosity and, therefore, to a lower BET surface area.

BET and XRD measurements showed that the surface areas of the UV and PC supports decreased after metal deposition and reduction with H_2 (300 °C, 2 h), accompanied by an increase of the crystallite size of TiO_2. A further morphological change toward the same direction was observed to occur after conditioning of the catalysts following the procedure described in the experimental section (15 min in He at 500 °C followed by exposure to the reaction mixture at 450 °C for 1 h). The above changes were more pronounced for the high surface area samples (UV, PC) and less significant or negligible for the low surface area samples (P25, AT) (Table 1).

An example of the effect of the above treatments on the XRD patterns of the materials is given in Fig. 2,

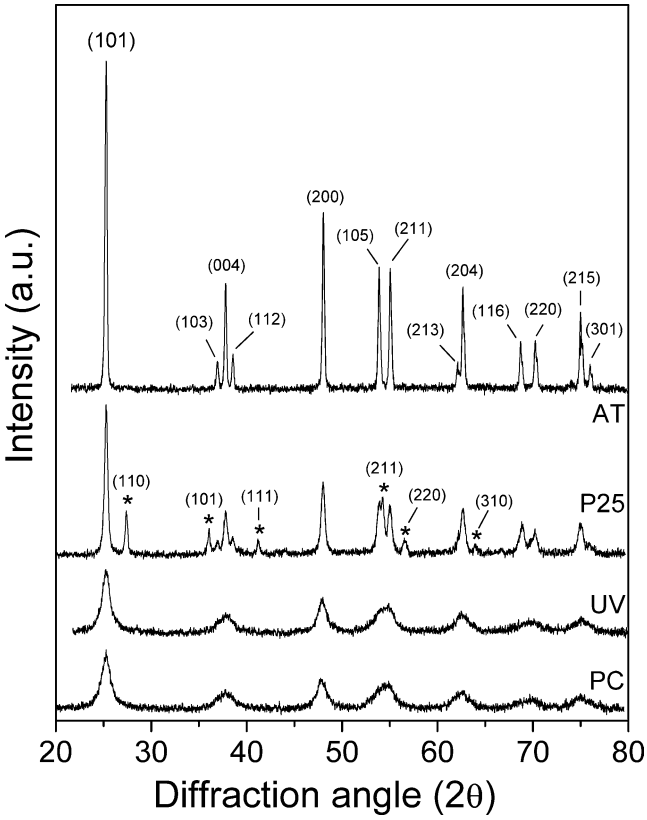

Fig. 1. X-ray diffractograms of commercial TiO_2 powders used as supports, with reflection planes of anatase and rutile (*) phases indicated.

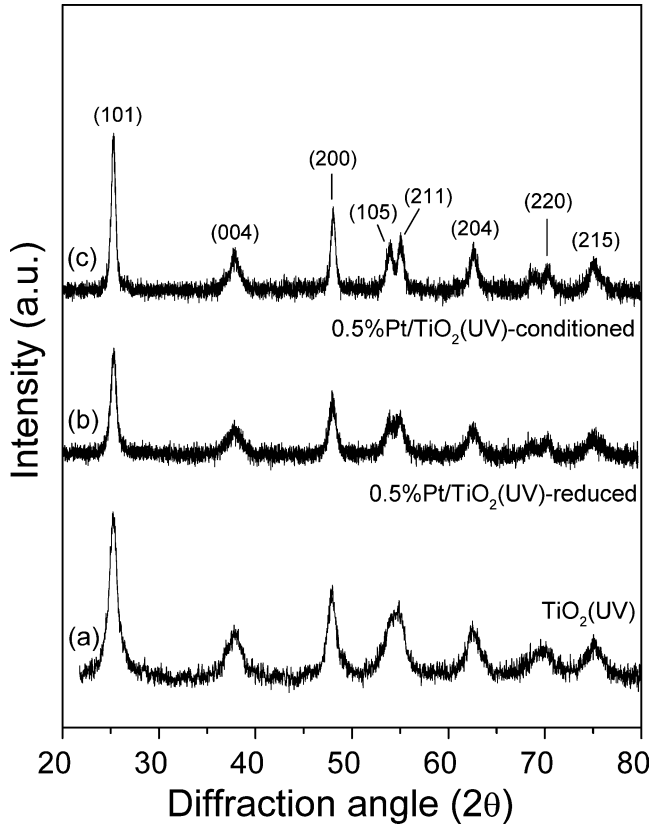

Fig. 2. X-ray diffractograms obtained from (a) the as-received TiO_2(UV) support, and from the reduced 0.5% Pt/TiO_2(UV) catalyst (b) before and (c) after conditioning at high temperature (see text).

Table 2
Physicochemical characteristics of M/TiO_2 catalysts and their activation energies for the WGS reaction

Catalyst	Metal loading (wt%)	Metal dispersion (%)	Metal crystallite size (Å)	Activation energy (kcal/mol)
Pt/TiO_2(P25)	0.1	72	14	15.7
	0.5	87	12	15.7
	2.0	52	20	16.4
	5.0	33	31	15.6
Ru/TiO_2(P25)	0.1	100	10	16.3
	0.5	46	21	15.7
	1.0	40	24	15.7
	2.0	29	32	14.2
	5.0	21	45	11.7
Rh/TiO_2(P25)	0.5	88	12	16.8
Pd/TiO_2(P25)	0.5	67	17	17.1
Pt/TiO_2(P25)				
600 °C (2 h)	2.0	28	37	16.8
600 °C (2 h)	5.0	8.8	115	15.6
650 °C (4 h)	5.0	6.4	160	17.5
700 °C (4 h)	5.0	6.3	162	17.3
Pt/TiO_2(UV)	0.5	14	73	11.9
Pt/TiO_2(PC)	0.5	62	16	12.4
Pt/TiO_2(AT)	0.5	47	22	16.9

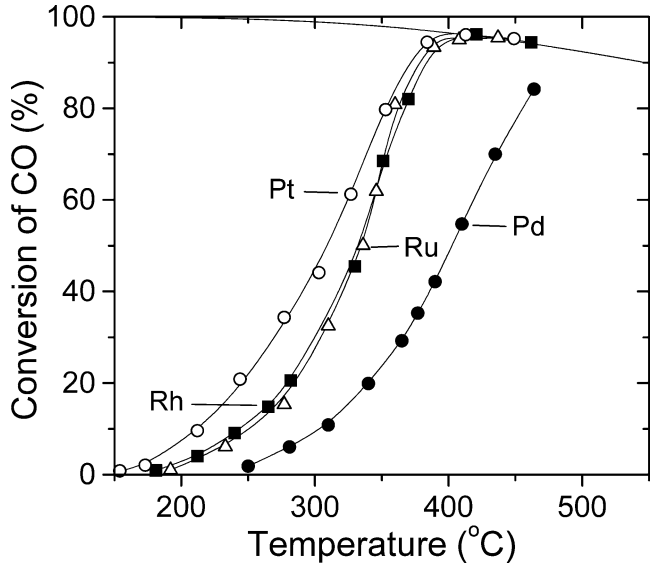

Fig. 3. Effect of reaction temperature on the conversion of CO obtained over Pt, Rh, Ru, and Pd catalysts (0.5 wt%) supported on TiO_2(P25). Mass of catalyst, 100 mg; particle diameter, $0.18 < d_p < 0.25$ mm; feed composition, 3% CO, 10% H_2O (balance He); total flow rate, 200 cm^3/min.

where the diffractogram of the as-received TiO_2(UV) carrier (trace a) is compared to those obtained after Pt deposition (trace b) and conditioning of the catalyst at high temperatures (trace c). It is observed that the above treatments resulted in an increase of the primary crystallite size of TiO_2 from 9 to 16 nm (Table 1), as evidenced by the narrowing of the XRD reflections and the increased resolution of neighboring peaks (e.g., of (105) and (211) planes). This was accompanied by a substantial change of the BET surface area of the material, which decreased from 238 to 71 m^2/g. It should be noted that similar measurements obtained over the "spent" catalysts showed that the morphological characteristics of the conditioned samples did not further change during kinetic measurements or catalytic performance tests. In all cases, the phase composition of TiO_2 did not change measurably. This is rather expected since temperatures typically higher than 600 °C are necessary for the transition of anatase to rutile.

The physicochemical characteristics of the various TiO_2-supported Pt, Ru, Rh, and Pd catalysts synthesized in the present study are summarized in Table 2.

3.2. WGS activity of dispersed noble metal catalysts

The effect of the nature of the dispersed metal on catalytic performance was investigated over noble metal catalysts with the same metal loading (0.5 wt%) supported on TiO_2(P25). Results are presented in Fig. 3, where the conversion of CO (X_{CO}) obtained over Pt, Rh, Ru, and Pd catalysts is plotted as a function of reaction temperature. The equilibrium conversion, predicted by thermodynamics, is also shown for comparison. It is observed that, under the experimental conditions employed, the Pt-loaded sample gives measurable conversions at temperatures above 150 °C. X_{CO} increases with increasing temperature and reaches equilibrium at ca. 400 °C. The conversion curves obtained from Rh and Ru catalysts are similar to each other but shifted toward higher temperatures, compared to that of Pt. The Pd catalyst is significantly less active than the other samples examined, giving measurable conversions above 250 °C, while temperatures higher than 450 °C are necessary to achieve equilibrium CO conversions (Fig. 3).

Turnover frequencies of CO conversion were determined from separate kinetic measurements obtained under differential reaction conditions, taking into account the results of selective chemisorption of H_2 (Table 2). Results are summarized in the Arrhenius-type diagram of Fig. 4, where the TOFs obtained from the catalysts examined are plotted as functions of reaction temperature. It is observed that catalytic activity depends appreciably on the nature of the dispersed metallic phase, and varies by a factor of 20 in the order of Pt > Rh > Ru > Pd. For example, the turnover frequencies measured at 250 °C are 0.46 s^{-1} for Pt, 0.16 s^{-1} for Rh, 0.07 s^{-1} for Ru, and 0.027 s^{-1} for Pd (Fig. 4). Different rankings of noble metals, with respect to their activity for the WGS reaction, have been reported in the literature. For example, Grenoble et al. [3] found that activity varies in the order of Ru > Pt > Pd ≈ Rh over Al_2O_3-supported catalysts, while Bunluesin et al. [15] reported that rates are essentially the same for CeO_2-supported Pt, Pd, and Rh catalysts. These differences may be attributed to the different nature of the oxide carriers used and/or, as will be discussed below, to the effect of the structural and morphological characteristics of the support on catalytic activity.

The apparent activation energies (E_a) of the WGS reaction over the four catalysts examined were calculated from

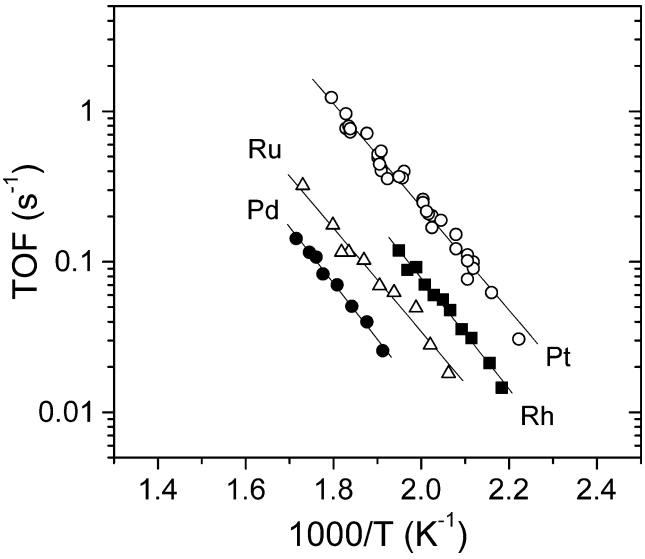

Fig. 4. Arrhenius plot of turnover frequencies of CO conversion obtained over Pt, Rh, Ru, and Pd catalysts (0.5 wt%) supported on TiO_2(P25).

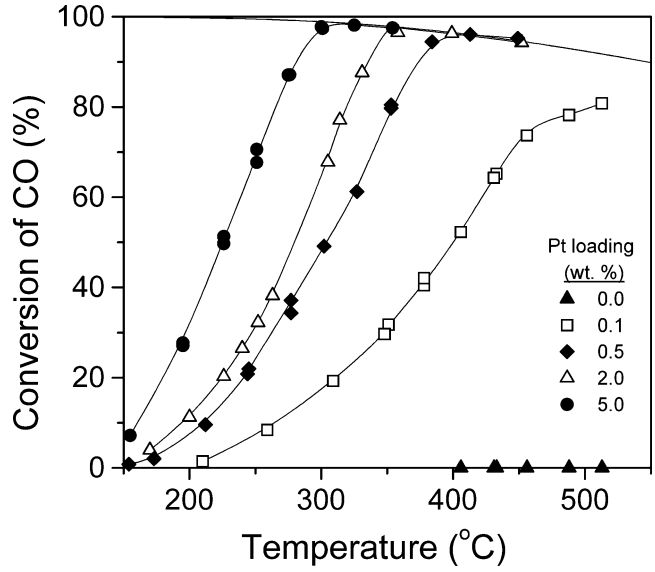

Fig. 5. Effect of metal loading on the catalytic performance of Pt catalysts supported on TiO_2(P25). Experimental conditions: same as in Fig. 3.

the slopes of the fitted lines shown in Fig. 4 and results are summarized in Table 2. It is observed that the activation energies are practically the same for this set of catalysts (0.5% M/TiO_2(P25)), taking values between 15.7 and 17.1 kcal/mol. This result indicates that, under the present reaction conditions, the activation energy does not depend on the nature of the metallic phase but, mainly, on the nature of the support. This is in accordance to the results of Grenoble et al. [3], who found that E_a varies in the range of 19.1–23.0 kcal/mol over Al_2O_3-supported Pt, Rh, Ru, and Pd catalysts and those of Bunluesin et al. [15] who reported activation energies of 11 ± 1 kcal/mol for CeO_2-supported Pt, Rh, and Pd catalysts.

3.3. Effect of metal loading and crystallite size on catalytic performance

The effect of metal loading on catalytic performance has been investigated over platinum and ruthenium catalysts (0–5 wt%) supported on TiO_2(P25). Results obtained from Pt/TiO_2 catalysts of variable metal loading are shown in Fig. 5. It is observed that the unmetallized support is practically inactive in the temperature range examined. However, addition of small amounts of Pt (0.1 wt%) results in a significant increase of activity for the WGS reaction. Further increase of Pt loading results in a progressive shift of the conversion curve toward lower temperatures. The 5% Pt/TiO_2 catalyst is active at temperatures lower than 150 °C and X_{CO} reaches equilibrium conversions at temperatures below 300 °C (Fig. 5).

Qualitatively similar results were obtained over Ru/TiO_2(P25) catalysts of variable Ru content (not shown for the shake of brevity). As in the case of Pt catalysts, conversion curves shift toward lower reaction temperatures with increasing Ru loading from 0.1 to 5.0 wt%. Comparison of

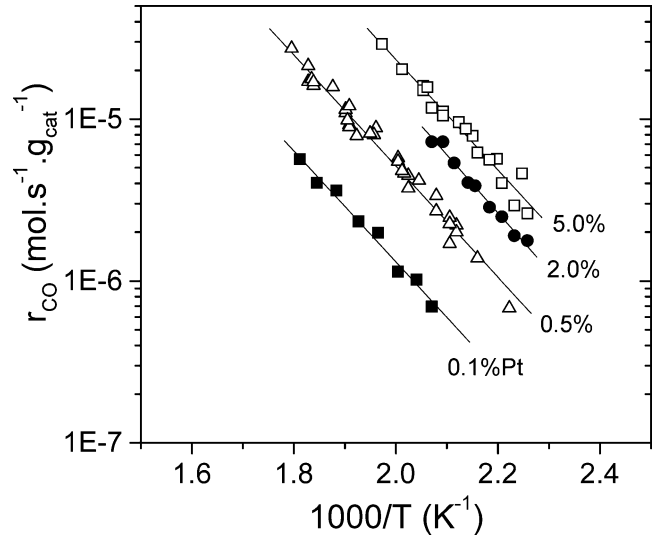

Fig. 6. Arrhenius plots of reaction rates obtained over Pt/TiO_2(P25) catalysts of variable metal loading.

the corresponding curves shows that, in general, Pt catalysts exhibit higher CO conversions at a given temperature, compared to Ru samples of the same metal loading.

Results of reaction rate measurements obtained over the Pt/TiO_2 samples of variable metal loading are shown in the Arrhenius-type diagram of Fig. 6. It is observed that reaction rates (per gram of catalyst) increase with increasing metal loading. The activation energies determined from the slopes of the fitted lines are summarized in Table 2. It is evident that the activation energy is practically independent of Pt loading. This is also the case for Ru/TiO_2 samples (Table 2).

Turnover frequencies calculated for the Pt/TiO_2(P25) catalysts of variable metal loading (0.1–5.0 wt%) lie on the same line (Fig. 7A), indicating that the specific activity of

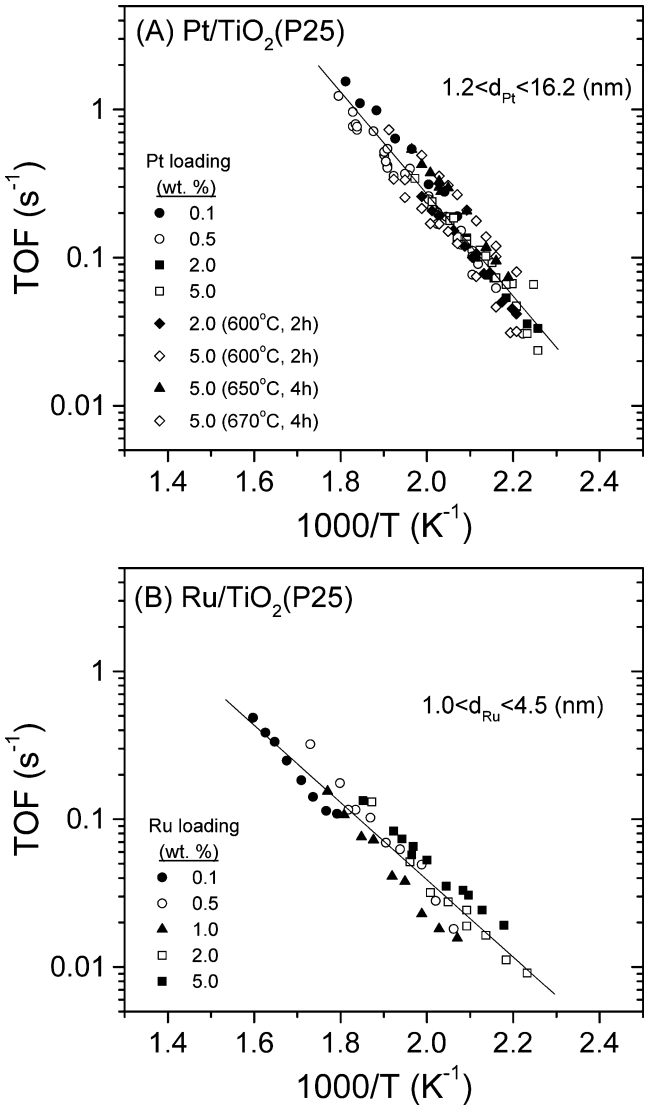

Fig. 7. Arrhenius plots of turnover frequencies (TOF) of CO conversion obtained over (A) Pt/TiO_2(P25) and (B) Ru/TiO_2(P25) catalysts of variable metal loading and metal crystallite size.

Pt does not depend on Pt loading or crystallite size. In order to confirm this observation, a second set of Pt/TiO_2(P25) catalysts was prepared by calcining portions of the 2% and 5% Pt/TiO_2 samples at high temperatures (600–700 °C) for a period of 2 or 4 h. The metal dispersions and mean crystallite sizes of these catalysts are listed in Table 2, and the measured TOFs are also plotted in Fig. 7A. It is observed that, within experimental error, the turnover frequencies of CO conversion are essentially the same for a given temperature, over a wide range of Pt crystallite sizes (1.2–16.2 nm).

Similar results obtained from the set of Ru/TiO_2(P25) catalysts of variable metal loading are shown in Fig. 7B. It is observed that, as in the case of the Pt catalysts, the TOF does not depend on Ru loading (0.1–5 wt%) or crystallite size (1.0–4.5 nm). Results of Figs. 7A and 7B provide strong evidence that reaction rates over titania-supported Pt and Ru do not depend on the morphological characteristics

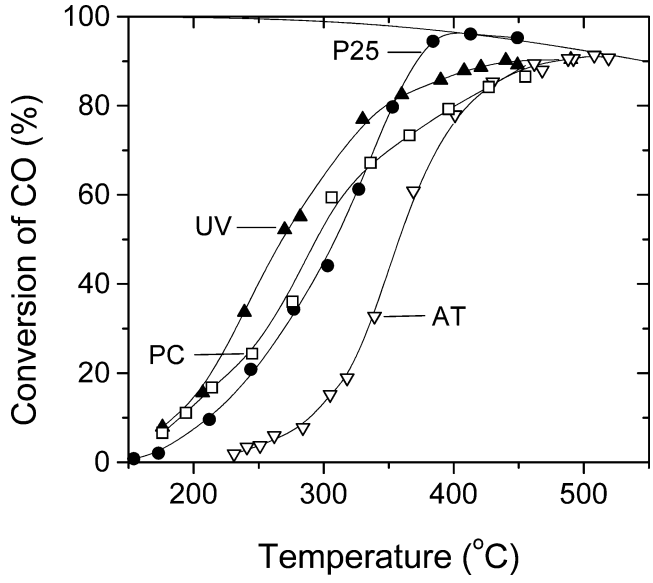

Fig. 8. Effect of the type of the TiO_2 support on the catalytic performance of Pt catalysts (0.5 wt%). Experimental conditions: same as in Fig. 3.

of the metallic phase but only on the amount of the exposed surface metal atoms. This finding is in accordance with the results of Grenoble et al. [3] who showed that the turnover rate of a number of metals supported on Al_2O_3 is essentially constant over a wide range of metal dispersions. Similarly, Wang et al. [16] demonstrated that the WGS rates on a series of Pd/ceria were strictly proportional to the Pd surface area.

3.4. Effect of morphological characteristics of the support

The effect of structural and morphological characteristics of the support on catalytic performance has been investigated over Pt catalysts with the same metal loading (0.5 wt%) dispersed on four different commercial TiO_2 carriers (Table 1), and results are shown in Fig. 8. It is observed that, when Pt is dispersed on TiO_2(AT), i.e., the carrier with the lowest surface area (largest TiO_2 crystallite size), the conversion curve shifts toward higher temperatures, compared to that of the Pt/TiO_2(P25) catalyst discussed above. In contrast, Pt catalysts supported on the high surface area (low TiO_2 crystallite size) samples exhibit higher CO conversions at low temperatures. However, the Pt/TiO_2(UV) and Pt/TiO_2(PC) catalysts are not able to reach equilibrium conversions at temperatures lower than 500 °C, under the present experimental conditions (Fig. 8).

Results of kinetic measurements obtained over the above set of catalysts at differential reaction conditions showed that the reaction rate (per gram of catalyst) depends strongly on the type of TiO_2 carrier used and increases with increasing surface area of the support or, conversely, with decreasing the primary particle size of TiO_2. For example, the rate at 250 °C increases by a factor of 20 going from 0.5% Pt/TiO_2(AT) (1.2 $\mu mol\, g^{-1}\, s^{-1}$) to 0.5% Pt/TiO_2(UV) (24.0 $\mu mol\, g^{-1}\, s^{-1}$). These differences become more pronounced if one compares the turnover frequencies deter-

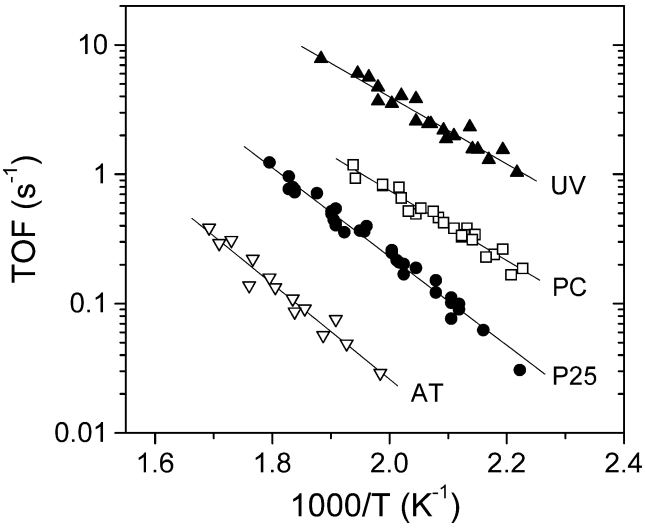

Fig. 9. Arrhenius plots of turnover frequencies obtained over Pt catalysts (0.5 wt%) supported on the indicated TiO_2 carriers.

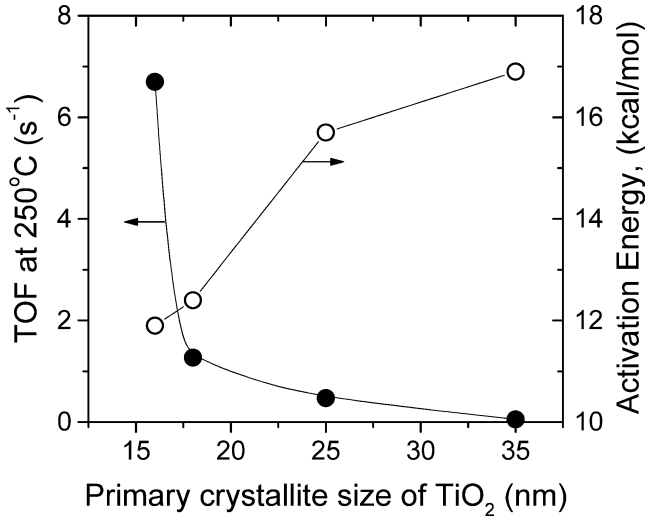

Fig. 10. Dependence of turnover frequency and activation energy of the WGS reaction over Pt/TiO_2 catalysts on the primary crystallite size of TiO_2.

mined for the above samples. As observed in Fig. 9, the reaction rate per surface Pt atom increases by more than two orders of magnitude (factor of 120 at 250 °C) going from the low surface (large TiO_2 crystallite size) to the high surface (small TiO_2 crystallite size) area samples. It is important to note that the activation energy of the reaction also varies depending on the TiO_2 support employed (Table 2) and decreases from 16.9 to 11.9 kcal/mol going from Pt/TiO_2(AT) to the Pt/TiO_2(UV) catalyst.

As has been shown above, the turnover frequency and the activation energy of the reaction do not depend on the crystallite size of Pt, for catalysts supported on the same type of TiO_2 carrier (Fig. 7A, Table 2). Therefore, the differences in TOF and E_a observed over the four 0.5% Pt/TiO_2 samples (Fig. 9) should be attributed to differences in the morphological characteristics of the supporting material. This dependence is clearly shown in Fig. 10, where the TOFs of CO conversion at 250 °C and E_a are plotted as functions of the primary crystallite size of TiO_2 (d_{TiO_2}). It should be noted that d_{TiO_2} refers to the crystallite size of the "spent" catalysts (Table 1). It is evident that decreasing the crystallite size of TiO_2 results in a dramatic increase of the activity of dispersed Pt, which is accompanied by a substantial decrease of the activation energy of the reaction. This is in accordance with the results of Bunluesin et al. obtained on Pd/CeO_2 catalysts [15]. These authors found that calcination of the ceria support at high temperatures, which was applied to increase crystallite size of the support, resulted in a decrease of the specific rate of Pd by a factor of 50 and in an increase of the activation energy of the reaction from 11 to 21 kcal/mol, compared to the catalyst calcined at low temperatures. However, in a following publication, the same group reported that the WGS rates were strictly proportional to the Pd surface area and that ceria crystallite size had no effect, at least for the range of ceria crystallite sizes between 7.2 and 40 nm [16].

3.5. Mechanistic implications

It is generally accepted that the WGS reaction occurs in a bifunctional manner, with the participation of both the dispersed metallic phase and the support. Two general mechanistic schemes have been proposed for the reaction over supported metal catalysts [4]: (a) the redox or "regenerative" mechanism, according to which CO adsorbed on the metal is oxidized by the support, which in turn is reoxidized by water [16], and (b) the "associative" mechanism which involves interaction of CO adsorbed on the metal with a hydroxyl group of the support and formation of a formate-type intermediate, which further decomposes to CO_2 and H_2 [19]. The applicability of the redox mechanism is by nature restricted to catalysts supported on "reducible" carriers and has been proposed to explain the high WGS activity of CeO_2-supported noble metals [16] as well as of Au/Fe_2O_3 and Au/TiO_2 catalysts [20]. However, recent investigations by Davis and co-workers [21,22] provided evidence which favors the formate intermediate mechanism on Pt/CeO_2 catalysts. In any case, most investigators agree that water adsorption and activation take place on the support while carbon monoxide adsorbs on the dispersed metal.

Results of the present study show that when Pt, Rh, Ru, or Pd is dispersed on the same type of TiO_2 support, the apparent activation energy of the reaction does not practically change, although the TOF of CO conversion varies by a factor of 20 going from Pt to Pd (Fig. 4). This implies that, under the present reaction conditions, the dominating contribution to the activation energy originates from a reaction step associated with the support (e.g., water adsorption/activation, surface reaction). This is evidenced by the observed dependence of activation energy on the type of titanium dioxide powder used as support (Fig. 10).

The role of the precious metal is most probably restricted to CO adsorption and supply to the metal–TiO_2 interface

where it either interacts with hydroxyl groups to form a formate intermediate (associative mechanism) and/or is oxidized by the reducible support to form CO_2 (redox mechanism). The observed ranking of metal activity (Pt > Rh > Ru > Pd) may then be correlated to the strength of the CO–metal bonds, as proposed by Grenoble et al. [3] who found a volcano-type relation between WGS activity of metals and their respective CO heats of adsorption. The relatively weak (factor of 20) dependence of the rate on the nature of the dispersed metal (Fig. 4) reflects the narrow range of strengths of CO interaction with the metals investigated.

The finding that TOF does not depend on the particle size of the dispersed metal (Fig. 7) is rather unexpected since one would argue that, for bifunctional catalysts, the active sites should be restricted to the metal–support interface. However, results of the present study show that this is not the case, at least for Pt/TiO_2 and Ru/TiO_2 catalysts (Fig. 7). The fact that the entire surface of the noble metal is effective for catalyzing the WGS reaction implies that the rates of transfer of catalytically active intermediate species to or from the support are fast, compared to the overall reaction rate.

Results presented in Figs. 8–10 clearly show that the key parameter which determines the WGS activity of Pt/TiO_2 catalysts is related to the physicochemical properties of the support. Since the observed dependence of catalytic activity on the type of TiO_2 used cannot be directly related to parameters such as surface area or anatase-to-rutile content, we choose to explain the results by considering the differences in the primary crystallite size of TiO_2. Assuming that the regenerative mechanism is operable, the observed strong dependence of TOF on the type of TiO_2 carrier employed may be related to the effect of crystallite size of TiO_2 on its redox properties. Calculations have shown that the reducibility of small oxide clusters depends on its size [23], as has been found, for example, in the case of ceria [23,24] and lanthana [25]. In a recent study of the WGS reaction on Pt/CeO_2 catalysts [21], it was shown that reducibility of surface ceria depends strongly on ceria domain size (particle size of CeO_2 crystallites) as well as on the degree of interaction with the noble metal. Interestingly, the exponential decrease of TOF observed in Fig. 10 with increasing d_{TiO_2} is qualitatively similar to the dramatic decrease of oxygen uptake, which is a measure of reducibility, observed with increasing the domain size of ceria in 1% Pt/CeO_2 catalysts [21]. It may then be suggested that the decreased activity observed for Pt/TiO_2 catalysts of the present study with increasing the primary particle size of the TiO_2 support is due to the decreased reducibility of larger titania crystallites.

It should be noted, however, that results may be explained equally well by taking into account the associative mechanism. This is because the morphological characteristics of the support may also influence the type, number, density, and reactivity of surface hydroxyl groups [26], which play a key role in the formation of formate-type intermediates [19,22,23]. It has been reported that the hydroxyl concentration in titania crystalline structures decreases with increasing crystallite size [27], which is in accordance with the observed effect of the support on catalytic activity (Fig. 10). Clearly, detailed mechanistic studies are necessary to elucidate the mechanism of the WGS reaction over TiO_2-supported noble metal catalysts.

4. Conclusions

The WGS activity of noble metals supported on TiO_2 has been investigated with respect to the structural and morphological characteristics of the dispersed metallic phase and the support. It has been found that, although the turnover frequency of CO conversion varies by a factor of 20 in the order of Pt > Rh > Ru > Pd, the activation energy of the reaction is essentially the same for all metals examined. Reaction rates, per gram of catalyst, increase significantly with increasing metal loading, resulting in a shift of the conversion curves toward lower temperatures. However, the activation energy of the reaction and rate per surface metal atom do not depend on the morphological characteristics of the metallic phase, such as loading, dispersion, and crystallite size.

Catalytic activity depends strongly on the structure and morphology of the support. The rate per surface Pt atom increases by more than two orders of magnitude with decreasing crystallite size of TiO_2 from 35 to 16 nm, with a parallel decrease of activation energy from 16.1 to 11.9 kcal/mol. This results in catalysts with higher activity at temperatures lower than 350 °C. It is concluded that TiO_2-supported noble metals with proper structural and morphological characteristics (high metal dispersion, small TiO_2 crystallite size) may be considered as promising candidates for the low-temperature WGS reaction for fuel cell applications.

Acknowledgments

This work was funded by the General Secretariat of Research and Technology (GSRT) Hellas and the Commission of the European Community, under the PENED 2001 Programm (Contract 01ED561).

References

[1] D.L. Trimm, Z.I. Önsan, Catal. Rev. 43 (2001) 31.
[2] A.F. Ghenciu, Curr. Opin. Solid State Mater. Sci. 6 (2002) 389.
[3] D.C. Grenoble, M.M. Estadt, D.F. Ollis, J. Catal. 67 (1981) 90.
[4] J. Barbier Jr., D. Duprez, Appl. Catal. B 3 (1993) 61.
[5] R. Dictor, J. Catal. 106 (1987) 458.
[6] Basińska, L. Kępiński, F. Domka, Appl. Catal. A 183 (1999) 143.
[7] S. Hilaire, X. Wang, T. Luo, R.J. Gorte, J. Wagner, Appl. Catal. A 215 (2001) 271.
[8] D. Andreeva, V. Idakiev, T. Tabakova, A. Andreev, R. Giovanoli, Appl. Catal. A 134 (1996) 275.
[9] D. Andreeva, V. Idakiev, T. Tabakova, L. Ilieva, P. Falaras, A. Bourlinos, A. Travlos, Catal. Today 72 (2002) 51.
[10] F. Boccuzzi, A. Chiorino, M. Manzoli, D. Andreeva, T. Tabakova, L. Ilieva, V. Iadakiev, Catal. Today 75 (2002) 169.
[11] Q. Fu, S. Kudriavtseva, H. Saltsburg, M. Flytzani-Stephanopoulos, Chem. Eng. J. 93 (2003) 41.

[12] Erdőhelyi, K. Fodor, G. Suru, Appl. Catal. A 139 (1996) 131–147.
[13] Y. Li, Q. Fu, M. Flytzani-Stephanopoulos, Appl. Catal. B 27 (2000) 179.
[14] J.M. Zalc, V. Sokolovskii, D.G. Löffler, J. Catal. 206 (2002) 169.
[15] T. Bunluesin, R.J. Gorte, G.W. Graham, Appl. Catal. B 15 (1998) 107.
[16] X. Wang, R.J. Gorte, J.P. Wagner, J. Catal. 212 (2002) 225.
[17] R.A. Spurr, H. Myers, Anal. Chem. 59 (1957) 761.
[18] B.D. Cullity, Elements of X-Ray Diffraction, Addison–Wesley, Reading, MA, 1978.
[19] T. Shido, Y. Iwasawa, J. Catal. 141 (1993) 71.
[20] F. Boccuzzi, A. Chiorino, M. Manzoli, D. Andreeva, T. Tabakova, J. Catal. 188 (1999) 176.
[21] G. Jacobs, L. Williams, U. Graham, G.A. Thomas, D.E. Sparks, B.H. Davis, Appl. Catal. A 252 (2003) 107.
[22] G. Jacobs, E. Chenu, P.M. Patterson, L. Williams, D. Sparks, G. Thomas, B.H. Davis, Appl. Catal. A 258 (2004) 203.
[23] H. Cordatos, D. Ford, R.J. Gorte, J. Phys. Chem. 100 (1996) 18128.
[24] H. Cordatos, T. Bunluesin, J. Stubenrauch, J.M. Vohs, R.J. Gorte, J. Phys. Chem. 100 (1996) 785.
[25] E.S. Putna, B. Sherek, R.J. Gorte, Appl. Catal. B 17 (1998) 101.
[26] C. Arrouvel, M. Digne, M. Breysse, H. Toulhoat, P. Raybaud, J. Catal. 222 (2004) 152.
[27] Bokhimi, A. Morales, O. Novaro, T. López, E. Sánchez, R. Gómez, J. Mater. Res. 10 (1995) 2788.